Robotica (2012) volume 30, pp. 145–157. © Cambridge University Press 2011
doi:10.1017/S0263574711000440

A framework for the analysis and synthesis of 3D dynamic human gait

Flavio Firmani* and Edward J. Park

Mechatronic Systems Engineering, School of Engineering Science, Simon Fraser University, 13450–102 Avenue, Surrey, BC V3T 0A3, Canada

(Received in Final Form: April 8, 2011. First published online: May 17, 2011)

SUMMARY

A comprehensive framework for the analysis and synthesis of 3D human gait is presented. The framework consists of a realistic morphological representation of the human body involving 40 degrees of freedom and 17 body segments. Through the analysis of human gait, the joint reaction forces/moments can be estimated and parameters associated with postural stability can be quantified. The synthesis of 3D human gait is a complicated problem due to the synchronisation of a large number of joint variables. Herein, the framework is employed to reconstruct a dynamically balanced gait cycle and develop sets of reference trajectories that can be used for either the assessment of human mobility or the control of mechanical ambulatory systems. The gait cycle is divided into eight postural configurations based on particular gait events. Gait kinematic data is used to provide natural human movements. The balance stability analysis is performed with various ground reference points. The proposed reconstruction of the gait cycle requires two optimisation steps that minimise the error distance between evaluated and desired gait and balance constraints. The first step (quasi-static motion) is used to approximate the postural configurations to a region close to the second optimisation step target while preserving the natural movements of human gait. The second step (dynamic motion) considers a normal speed gait cycle and is solved using the spacetime constraint method and a global optimisation algorithm. An experimental validation of the generated reference trajectories is carried out by comparing the paths followed by 19 optical markers of a motion tracking system with the paths of the corresponding node points on the model.

KEYWORDS: Human biomechanics; Bipeds; Legged robots; Humanoid robots; Robot dynamics; Path planning.

1. Introduction

Biomechanical models of the human body are usually employed to estimate quantities that cannot be measured, such as the joint reaction forces and moments.[1] In addition, these models can also be employed to synthesise trajectories of mechanical ambulatory systems[2] and human motion.[3] The complexity of the model depends on the number of degrees of freedom (DOF) that are considered to represent the human body. Several kinematic models have been proposed in the literature, from simple linkages acting on the sagittal plane to more complex (three-dimensional) 3D models that can be employed to analyse human movements.[4] In this paper, our goal is to develop a framework that can be used for the analysis and synthesis of human gait. In general, a morphologically realistic model is not required for the analysis problem, as the significant points remain invariant with the body reference frames, e.g. locations of the centre of mass and the joint rotation centre. However, for the synthesis problem, the model interacts with the exterior, which is described with respect to an inertial reference frame. Therefore, it is necessary to model the human segments with anatomical shapes to ensure full knowledge of their interaction with the exterior, e.g. collision detection with the ground or obstacles. Thus, the proposed framework must contain a large number of DOF and also a realistic morphological representation of the human body segments.

Three-dimensional human gait synthesis is a complicated problem due to the synchronisation of a large number of joint variables. A critical problem in robotics is to synthesise gait trajectories that form the reference for controlling the motion of mechanical bipeds.[5] These reference trajectories, which are related to the displacement of each joint, must ensure the balance of the biped by satisfying a stability criteria pertaining to the interaction of the biped with the ground. A technique used for the generation of these trajectories is based on numerical optimisation algorithms[2] and involves a relatively complex dynamic model of the bipedal system. It is possible to use a complex model of the human body because the trajectories are determined offline and computation time is not an issue. This technique is generally robust as long as external conditions, such as terrain, obstacles and external forces, do not critically affect the stability of the biped. The reference trajectories can also be employed to assess human motion by comparing what would be a 'normal' type of motion in relation to a subject. For example, during the gait cycle, a series of events occur in regards to the posture of the individual and the interaction with the ground. An early or delayed occurrence of these events would indicate gait abnormalities.[6] Thus, these reference trajectories can be used to establish optimal rehabilitation strategies.

The proposed comprehensive framework was developed to analyse and synthesise human gait and other human movements. In particular, this paper focuses on the

* Corresponding author. E-mail: ffirmani@me.uvic.ca

reconstruction of normal human gait while providing balance stability and smooth motion. To this end, a complex morphological 3D human model that consists of 34 internal DOF and 6 external DOF is employed. The analysis of balance stability includes a set of ground reference points (GRPs), namely the projected Centre of Mass (pCM), Zero Moment Point (ZMP) and Centroidal Moment Pivot (CMP). The complete trajectory of the human body segments (displacement, velocity and acceleration) is generated with polynomial splines, providing smooth motion patterns.

The reconstruction of the dynamically balanced human gait cycle is carried out by optimising the joint displacements of eight postural configurations subject to some gait and balance constraints that happen during the gait cycle. The gait constraints are related to the interaction of the plantar surface with the ground, step width, foot angle and among others; whereas the balance constraints are specific profiles of GRPs.[7] Given that the model contains a large number of DOF, there are an infinite number of joint displacements that would satisfy the gait and balance constraints. Nevertheless, the objective for the reference trajectories is to preserve natural human movements. For the synthesis problem, the contribution of this work to the literature is the development of a two-step optimisation technique that converts generic gait kinematics into dynamically balanced postural configurations. In the first step, gait constraints are introduced and the postural configurations are optimised under slow walking conditions (quasi-static motion); thus, the gravitational forces are considerably greater than the inertial forces. By doing so, a balance constraint based on the profile of the pCM throughout the gait cycle is established. In the second optimisation step, normal walking speed (dynamic motion) is considered, and thus, the resulting inertial forces affect the human balance. The balance constraint is based on following a profile of the Centre of Pressure (CoP) by evaluating the ZMP. The dynamic motion is determined by using the spacetime constraint method[8] and a global optimisation algorithm. In both optimisation steps, the objective function minimises the error distance between evaluated and desired gait and balance constraints. The reason why two optimisation steps are proposed is because if only one step was considered, the optimisation algorithm would start from a set of joint displacements that are far from the target region, and consequently, it would find some solutions that alter the natural flow of the gait motion. The importance of the first optimisation step is the generation of a set of joint displacements that are close enough to the dynamically balance postures, and therefore, the natural movements of the gait cycle will be preserved. Finally, the computed reference trajectories are compared with experimental results. The comparison indicates that the path followed by node points on the model are contained within the region of the optical tracking marker paths.

2. Biomechanical Model

2.1. Kinematics

The human skeletal system is extremely complex. Zatsiorsky[9] estimates that there are 148 movable bones and 147 joints in the human body, yielding 244 DOF. The proposed model contains the most significant 17 body segments and 16 joints, totalling 34 internal DOF. In addition, there are 6 external DOF that describe the position and orientation of the pelvis with respect to an inertial reference frame. The spine is divided into three segments (pelvis, thorax/abdomen and neck/skull), and these segments are connected at the sacroiliac and cervical joints, both of which are modelled as 3-DOF joints. The lower limbs are modelled with four segments (thigh, shank, hind-mid foot and forefoot), which are connected with four joints totalling 7 DOF: hip joint (3 DOF), knee joint (1 DOF), ankle joint (1 DOF) and foot joints (2 DOF), which comprises the subtalar and metatarsophalangeal (MTP) joints. The upper limbs are also modelled with 7 DOF each: shoulder joint (3 DOF), elbow joint (1 DOF), radioulnar joint (1 DOF) and the wrist joint (2 DOF). The biomechanical analysis and the Denavit and Hartenberg (DH) parameters of this model are described in detail in our previous work.[10] Figure 1 shows the layout of the kinematic model.

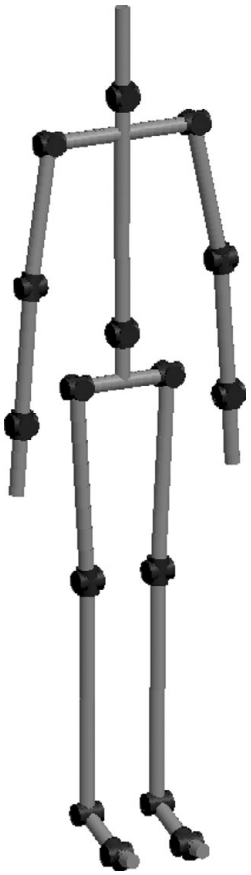

Fig. 1. Joint layout model.

2.2. Morphological 3D human representation

In order to create a framework that can be used for the synthesis of human motion, it is necessary to develop a morphological 3D human model that offers a more realistic representation of the body segments and their interaction with the exterior. Ground collisions are considered to be perfectly inelastic. The generation of the support polygon,

https://doi.org/10.1017/S0263574711000440 Published online by Cambridge University Press

defined as the convex hull of the foot-support area commonly used in postural stability analysis of humanoid robots, is determined by enclosing all the node points that are in contact with the ground. In addition, the node points can also be used to create the gait constraints that are used to generate the postural configurations of the synthesis problem. The human body model is based on a Matlab open source graphic interface, in the form of a wireframe, created by Tordoff and Mayol[11] (original version in VRML by Cindy Ballreich). The wireframe model consists of a collection of body segments formed with node points, which are enclosed by polygons. In order to animate the human model, the authors modified the location of the node points by placing the proximal joint centre at the origin of an inertial reference frame and aligning the segment along the x- or z-axis depending on the definition of the segment, i.e. link length or link offset. The position and orientation of a body segment in space are defined by a homogeneous transform matrix based on the DH parameters; thus, the motion of the segments can be achieved by varying the joint angles. To improve the computation time of the animation, segments were converted into Matlab objects, and with the aid of handle graphics, the new posture of the segment in space is efficiently regenerated. Furthermore, the appearance of the model was improved by using the Matlab functions that allow to render graphics objects, including texture, light and reflection. Figure 2 shows the human body model in its zero-displacement configuration posture.

Fig. 2. (Colour online) Morphological 3D human model.

2.3. Anthropometric parameters

In order to evaluate dynamic quantities, a reasonable estimation of anthropometric parameters of each body segment is required. Herein, the results obtained by Zatsiorsky *et al.*[12] and later adjusted by De Leva[13] are employed. The former employed a gamma-ray scanner but used unconventional landmarks. The latter adjusted these values to the more conventional joint centres and reported the centre of mass location and radii of gyration as a percentage of the longitudinal length of each segment.

2.4. Inertial forces and moments

The inertial forces and moments can be determined as a function of joint quantities using the outward iteration of the double recursive Newton–Euler formulation.[14] The iteration begins from the first link frame and moves successively to the last link as the velocities and accelerations propagate. Velocities and accelerations are evaluated and employed to determine the inertial forces and moments acting at the body segment centre of mass. The initial conditions of the algorithm (the angular velocity, angular acceleration and linear acceleration of the pelvis in addition to gravity) are entered in the iteration as ${}^{Pv}\boldsymbol{\omega}_{Pv} = [\dot{\phi},\ \dot{\varphi},\ \dot{\psi}]^{\mathrm{T}}$, ${}^{Pv}\dot{\boldsymbol{\omega}}_{Pv} = [\ddot{\phi},\ \ddot{\varphi},\ \ddot{\psi}]^{\mathrm{T}}$ and ${}^{Pv}\dot{\mathbf{v}}_{Pv} = [\ddot{x} + g_x,\ \ \ddot{y} + g_y,\ \ \ddot{z} + g_z]^{\mathrm{T}}$, respectively.

$$
\begin{aligned}
\text{Angular Velocity of } i+1\text{:} \quad & {}^{i+1}\boldsymbol{\omega}_{i+1} = {}^{i+1}_{i}\mathbf{R}\,{}^{i}\boldsymbol{\omega}_{i} + \dot{\theta}_{i+1}\,{}^{i+1}\hat{\mathbf{z}}_{i+1}.\\
\text{Angular Acceleration of } i+1\text{:} \quad & {}^{i+1}\dot{\boldsymbol{\omega}}_{i+1} = {}^{i+1}_{i}\mathbf{R}({}^{i}\dot{\boldsymbol{\omega}}_{i} + {}^{i}\boldsymbol{\omega}_{i} \times \dot{\theta}_{i+1}\,{}^{i+1}\hat{\mathbf{z}}_{i+1}) + \ddot{\theta}_{i+1}\,{}^{i+1}\hat{\mathbf{z}}_{i+1}.\\
\text{Linear Acceleration of } i+1\text{:} \quad & {}^{i+1}\dot{\mathbf{v}}_{i+1} = {}^{i+1}_{i}\mathbf{R}({}^{i}\dot{\mathbf{v}}_{i} + {}^{i}\dot{\boldsymbol{\omega}}_{i} \times {}^{i}\mathbf{P}_{i+1} + {}^{i}\boldsymbol{\omega}_{i} \times ({}^{i}\boldsymbol{\omega}_{i} \times {}^{i}\mathbf{P}_{i+1})).\\
\text{Linear Acceleration of } G_{i+1}\text{:} \quad & {}^{i+1}\dot{\mathbf{v}}_{G_{i+1}} = {}^{i+1}\dot{\mathbf{v}}_{i+1} + {}^{i+1}\boldsymbol{\omega}_{i+1} \times ({}^{i+1}\boldsymbol{\omega}_{i+1} \times {}^{i+1}\mathbf{P}_{G_{i+1}}) + {}^{i+1}\dot{\boldsymbol{\omega}}_{i+1} \times {}^{i+1}\mathbf{P}_{G_{i+1}}.\\
\text{Inertial Force:} \quad & {}^{i+1}\mathbf{F}_{i+1} = m_{i+1}\,{}^{i+1}\dot{\mathbf{v}}_{G_{i+1}}.\\
\text{Inertial Moment:} \quad & {}^{i+1}\mathbf{N}_{i+1} = {}^{c_{i+1}}\mathbf{I}_{i+1}\,{}^{i+1}\dot{\boldsymbol{\omega}}_{i+1} + {}^{i+1}\boldsymbol{\omega}_{i+1} \times {}^{c_{i+1}}\mathbf{I}_{i+1}\,{}^{i+1}\boldsymbol{\omega}_{i+1}.
\end{aligned}
$$

---

3. Postural Stability

Postural stability is the ability to return to equilibrium after being perturbed. GRPs are employed to evaluate postural balance of human locomotion and ambulatory mechanical systems. The evaluation of GRP can be used for the assessment of gait patterns, control of legged robots and synthesis of gait motion. The CoP is commonly employed to assess

https://doi.org/10.1017/S0263574711000440 Published online by Cambridge University Press

gait patterns and is measured with force plates. The CoP is associated with the forces exerted by the foot-ground contact, which can be represented by a field of pressure forces. The CoP represents the point on the ground where the resultant of the forces normal to the contact surface acts; thus, no moment about this point is produced by the normal forces. A general definition of CoP involving frictional tangential forces is described as the point on the ground where the resultant of the field of pressure forces acts and only a tangential resultant moment exists. Statistical quantities of the coordinates of the CoP over time have been proposed to evaluate postural stability.[15] Under static or dynamically balanced conditions, the CoP must remain within the convex hull of the foot-support area (i.e. the support polygon) to maintain balance.

The remaining GRPs, i.e. pCM, ZMP and CMP, are not measurable quantities but can be calculated based on kinematic and anthropometric models. The kinematic data of the body segments are measured with optical motion caption systems or body-mounted sensors. Under static conditions, the sufficient condition to conclude that the biped (biological or mechanical) is in static equilibrium is to have the pCM inside the support polygon. The pCM exiting the support polygon indicates the existence of an unconstrained moment that causes the foot to rotate about a point on the edge of the support polygon leading to an unbalanced state that may result in a fall.

During dynamic conditions, inertial forces and moments caused by the accelerations of the body segments have to be considered for the balance analysis. The ZMP is associated with the forces exerted by the body segments due to gravity and accelerations. Dasgupta and Nakamura[7] defined the ZMP as the point on the ground at which the net moment of the inertial forces and the gravity forces has no component along the horizontal axes. The net moment about the ZMP described with respect to an inertial reference frame {0} can be determine as follows:

$$\sum_{i=1}^{n} \left(\left({}^{0}\mathbf{P}_{G_i} - {}^{0}\mathbf{P}_{ZMP} \right) \times m_i \, {}^{0}\mathbf{a}_{G_i} + {}^{0}\mathbf{I}_i \, {}^{0}\boldsymbol{\alpha}_i + {}^{0}\boldsymbol{\omega}_i \times {}^{0}\mathbf{I}_i \, {}^{0}\boldsymbol{\omega}_i \right) = [0, \, 0, \, *]^{\mathrm{T}}, \tag{1}$$

where the term ${}^{0}\mathbf{P}_{G_i} - {}^{0}\mathbf{P}_{ZMP}$ describes the position vector from $\mathbf{P}_{ZMP} = [X_{ZMP}, Y_{ZMP}, Z_{ZMP}]^{\mathrm{T}}$ to the centre of mass of the ith body segment $\mathbf{P}_{G_i} = [X_{G_i}, Y_{G_i}, Z_{G_i}]^{\mathrm{T}}$, and ${}^{0}\mathbf{a}_{G_i}$ already includes the effect of gravity and $*$ represents a non-zero quantity. The above equation may be rewritten in terms of inertial forces and moments, i.e.

$$\sum_{i=1}^{n} \left(\left({}^{0}\mathbf{P}_{G_i} - {}^{0}\mathbf{P}_{ZMP} \right) \times {}^{0}\mathbf{F}_{G_i} + {}^{0}\mathbf{N}_i \right) = [0, \, 0, \, *]^{\mathrm{T}}, \tag{2}$$

yielding the following ZMP coordinates:

$$X_{ZMP} = \frac{\sum \left(X_{G_i} \cdot F_{i_z} - Z_{G_i} \cdot F_{i_x} - N_{i_y} \right)}{\sum F_{i_z}}, \qquad Y_{ZMP} = \frac{\sum \left(Y_{G_i} \cdot F_{i_z} - Z_{G_i} \cdot F_{i_y} + N_{i_x} \right)}{\sum F_{i_z}}. \tag{3}$$

It is worth mentioning that despite the conceptual difference between CoP (based on contact forces) and ZMP (based on gravity and inertial forces), these two points are always coincident during dynamically balanced gait,[16] as both points involve zero moments about the horizontal axes. A detailed comparison of these ground reference points is presented in ref. [17]. The only debatable difference occurs when the gait is not dynamically balanced, as the CoP acts at the edge of the rolling foot (no longer a contact surface), a rotation caused by an unconstrained moment, whereas the ZMP does not exist because the horizontal component of the moment is no longer zero.

The CMP, also referred to as Zero Rate of Angular Momentum,[18] measures rotational postural stability based on evaluating the angular momentum of the whole body about the CM. A biped is said to be rotationally stable if the external forces and moments sum up to a zero centroidal moment,[18] i.e. $\dot{\mathbf{H}}_G = 0$. To satisfy this condition, the resultant reaction force must pass through the CM; otherwise, an unconstrained moment is created. The CMP is defined as the point where the ground reaction force would have to act to keep the horizontal component of the whole body angular momentum constant.[19] The CMP coordinates written in terms of the ground reaction force and the CM are

$$X_{CMP} = X_{CM} - \frac{\sum F_{i_x}}{\sum F_{i_z}} Z_{CM}, \qquad Y_{CMP} = Y_{CM} - \frac{\sum F_{i_y}}{\sum F_{i_z}} Z_{CM}. \tag{4}$$

For the development of reference trajectories, profiles of a dynamically balanced CoP are used. For the synthesis problem, eight postural configurations are to be optimised. Therefore, a correlation during the gait cycle between the postures and the CoP profiles was made. The points on the CoP profiles that correspond to the eight postural configurations will be used as the balance constraints in the optimisation problem.

There is an instance during the gait cycle when the human body experiences an unbalanced situation, this occurs when the weight is transferred from one foot to the other. In this case, the CoP is located at the edge of the rolling foot and the postural stability criteria given by the CoP is no longer valid. However, for our problem, none of the eight postural configurations occur during the unbalanced period, and therefore, the postural stability given by the CoP profile is preserved. During the unbalance situation, the swinging foot continues its motion until the heel strikes the ground returning to a dynamically balanced gait motion.

Once the balance constraints are identified, the joint displacements, which are the design variables of the optimisation problem, are varied to determine the postural configurations. The trajectory between each postural configuration is generated and the inertial forces/moments calculated. The ZMP is evaluated and used as the parameter that has to be approximated to the balance constraint derived from the CoP profile. This is possible because the CoP and ZMP are always coincident during dynamically balanced gait. Note that when a new postural configuration

https://doi.org/10.1017/S0263574711000440 Published online by Cambridge University Press

Table I. Periods of human gait cycle.

Period	Name	Duration	Right foot	Left foot
I	Loading response	*0–12.5%*	Heel strike – foot flat	MTP flexion – toe off
II	Initial single stance	*12.5–25%*	Foot flat	Toe off – feet adjacent
III	Midstance	*25–37.5%*	Foot flat – heel off	Feet adjacent – vertical tibia
IV	Terminal stance	*37.5–50%*	Heel off – MTP flexion	Vertical tibia – heel strike
V	Push off	*50–62.5%*	MTP flexion – toe off	Heel strike – foot flat
VI	Initial swing	*62.5–75%*	Toe off – feet adjacent	Foot flat
VII	Midswing	*75–87.5%*	Feet adjacent – vertical tibia	Foot flat – heel off
VIII	Terminal swing	*87.5–100%*	Vertical tibia – heel strike	Heel off – MTP flexion

is created, the trajectory generator outputs another set of joint velocities and accelerations, changing the value of the inertial forces/moments and consequently the location of the ZMP.

4. Gait Cycle

Human gait synthesis is a complex problem due to the synchronisation and coordination of a large number of DOF. When the mobility of one of the joints is affected, it influences the motion of the rest.[20] Consequently, the majority of the human gait models is constrained to the sagittal plane, neglecting the contribution of the joint motions/torques on the frontal and transverse planes. This assumption could critically affect the overall postural stability. Different strategies for gait synthesis have been proposed: Fourier series,[7] coupled oscillators[20] and polynomial splines.[21] Herein, polynomial splines are employed to reconstruct the gait cycle and this includes displacement of all seven joints of the leg, rotation of the sacroiliac joint, rotation of the arms on the sagittal plane (shoulder and elbow) and rotation and orientation of the pelvis in space. The motion trajectory of the human joints is generated with quintic polynomial splines by connecting via points the postural configurations.

4.1. Standard gait cycle

Normal walking is a repetitive series of movements. Each cycle initiates when the leading foot (right foot by convention) contacts the ground and concludes when the same foot contacts the ground after both feet have taken a step forward. During this time, a series of events take place regarding the position of the ipsilateral (right) and contralateral (left) lower limbs. The gait cycle is divided into two phases – stance and swing. The stance and swing phases correspond to approximately 62 and 38% of the gait cycle, respectively. This ratio changes depending on the speed of the walker. The gait cycle is generally divided into seven periods. The *loading response* period initiates when the ipsilateral foot contacts the ground and ends when the contralateral foot leaves the ground (toe off) at 10-12% of the gait cycle.[22] *Midstance* is referred to the period in which the right foot stays flat on the ground and ends when the ipsilateral heel rises, the timing of this event varies considerably among individuals, at 32% as reported in ref. [22] and at 40% as reported in ref. [23]. *Terminal stance* begins when the heel rises and ends when the contralateral foot contacts the ground at 50% of the gait cycle. *Push off* or *pre-swing* occurs from contralateral contact to ipsilateral toe off at 62% of gait cycle. *Initial swing* takes place from ipsilateral toe off to the moment when both feet are adjacent at around 75% of the gait cycle.[23] *Midswing* happens from both feet being adjacent to the moment when the swinging tibia is vertical at around 87% of the gait cycle.[23] *Final swing* occurs from the tibia being vertical to the heel striking the ground once again.

Due to the symmetry of both feet movements, the *midstance* period may be divided into two parts (*initial single stance* and *midstance*) to include the event in which the swinging left foot passes next to the right foot at around 25% of the gait cycle. In doing so, it was noted that the events occurred approximately in intervals of the same duration, i.e. 12.5% of the gait cycle, as shown in Table I.

Preliminary movements of the joint displacements are determined based on standard kinematic gait data reported by kinesiologists. This includes 27 joint displacement: all seven joints of the leg, rotation of the sacroiliac joint, rotation of the arms on the sagittal plane (shoulder and elbow) and rotation and orientation of the pelvis in space. Given that the pelvis is the 'reference' body segment, its motion is described relative to an inertial reference frame. In this work, an individual walking on a treadmill at normal speed is considered. Zhao *et al.*[24] reported complete 3D motion of the pelvis during a gait cycle on a treadmill. The gait kinematics of the remaining body segments are described relative to the proximal joint. Neumann[23] reported joint displacements of the right leg in all three planes. This includes joint angular rotation of the hip, knee and ankle joints in the sagittal plane, hip and subtalar angular motion in the frontal plane and hip rotation in the transversal plane. The MTP joint rotation is reported in ref. [25] and the sacroiliac rotation about all three axes is found in ref. [26], whereas the shoulder and elbow rotations in the sagittal plane are reported in ref. [6].

4.2. Trajectory generation

The smoothness of a joint motion trajectory can be quantified as a function of jerk. Shadmehr and Wise[27] demonstrated that a trajectory function that happens to have its sixth derivative equal to zero will minimise the jerk function. Thus, if polynomial functions are used, a fifth-order polynomial is

https://doi.org/10.1017/S0263574711000440 Published online by Cambridge University Press

the highest degree that will satisfy this condition. Polynomial schemes are broadly used in robotics to represent the trajectory of one joint that has to move from one configuration to another in a certain time period. Cubic[21] and quartic[28] polynomials have been employed to generate locomotion trajectories.

In order to approximate more accurately the profile of a joint displacement, the profile is divided into n segments and each segment is mathematically modelled with a polynomial. In this work, the overall profile is divided into eight segments in relation to the eight periods of the gait cycle as described in Table I. The first seven segments connect the eight postural configurations at the beginning of each period and the last segment connects the eighth with the first postural configurations to complete the gait cycle. The time derivatives of these polynomials yield the velocity, acceleration and jerk profiles.

The selection of the polynomial degree depends on the number of motion conditions that have to be satisfied. Each polynomial must satisfy the initial (i) and final (ii) positions of each joint resulting in two conditions. The final velocity and acceleration of one segment must be equal to the initial conditions of the next segment. Matching velocities (iii) and accelerations (iv) yield two more conditions. There are $m+1$ coefficients in an m-order polynomial; therefore, a cubic polynomial (four coefficients) could satisfy all four conditions; however, the jerk profile would be discontinuous. To provide a better smoothness higher order polynomials must be considered. Quartic polynomials could solve this problem; however, after testing the scheme problems of rank deficiency were experienced. Thus, quintic polynomials are chosen instead allowing two additional conditions to be satisfied, i.e. matching jerks (v) and jounces (vi) between segments. The quintic polynomial of the kth segment has the following structure:

$$q(t_k) = a_{0_k} + a_{1_k}t_k + a_{2_k}t_k^2 + a_{3_k}t_k^3 + a_{4_k}t_k^4 + a_{5_k}t_k^5. \quad (5)$$

Equations that described the motion conditions can be expressed, in general form, in terms of the kth segment as follows:

Initial position q_{0_k}:
$q_{0_k} = a_{0_k}$, with $t_k = 0$.

Final position q_{f_k}:
$q_{f_k} = a_{0_k} + a_{1_k}t_{f_k} + a_{2_k}t_{f_k}^2 + a_{3_k}t_{f_k}^3 + a_{4_k}t_{f_k}^4 + a_{5_k}t_{f_k}^5$, with $t_k = t_{f_k}$.

Matching velocities $\dot{q}_{f_k} = \dot{q}_{0_{k+1}}$:
$a_{1_k} + 2a_{2_k}t_{f_k} + 3a_{3_k}t_{f_k}^2 + 4a_{4_k}t_{f_k}^3 + 5a_{5_k}t_{f_k}^4 = a_{1_{k+1}}$, with $t_k = t_{f_k}$ and $t_{k+1} = 0$.

Matching accelerations $\ddot{q}_{f_k} = \ddot{q}_{0_{k+1}}$:
$2a_{2_k} + 6a_{3_k}t_{f_k} + 12a_{4_k}t_{f_k}^2 + 20a_{5_k}t_{f_k}^3 = 2a_{2_{k+1}}$, with $t_k = t_{f_k}$ and $t_{k+1} = 0$.

Matching jerks $\dddot{q}_{f_k} = \dddot{q}_{0_{k+1}}$:
$6a_{3_k} + 24a_{4_k}t_{f_k} + 60a_{5_k}t_{f_k}^2 = 6a_{3_{k+1}}$, with $t_k = t_{f_k}$ and $t_{k+1} = 0$.

Matching jounces $\ddddot{q}_{f_k} = \ddddot{q}_{0_{k+1}}$:
$24a_{4_k} + 120a_{5_k}t_{f_k} = 24a_{4_{k+1}}$, with $t_k = t_{f_k}$ and $t_{k+1} = 0$.

The gait cycle is modelled with eight segments; therefore, there are 48 conditions to be satisfied, i.e. 16 conditions for the initial and final positions and 32 conditions for matching time derivatives. Since the equations of the matching time derivatives involve coefficients of different segments (k and $k+1$), a system of 48 linear equations results, which can be written in matrix form as $\mathbf{Cx} = \mathbf{b}$, where $\mathbf{x}$ is a vector that includes all the unknown coefficients of the polynomials; whereas $\mathbf{C}$ and $\mathbf{b}$ are a square matrix and a vector, respectively. The elements of the $\mathbf{C}$ matrix are shown below:

Position $i = 2(s-1)+1$ and $j = 6(s-1)+1$, with $s = 1 : n-1$.
Initial position: $c_{i,j} = 1$.
Final position: $c_{i+1,j} = 1$, $c_{i+1,j+1} = t_{f_k}$, $c_{i+1,j+2} = t_{f_k}^2$, $c_{i+1,j+3} = t_{f_k}^3$, $c_{i+1,j+4} = t_{f_k}^4$, $c_{i+1,j+5} = t_{f_k}^5$.
Time derivatives $i = 4(s-1)+2(n-1)+1$, $j = 6(s-1)+1$ and $s = 1 : n-1$.
Velocities: $c_{i,j+1} = 1$, $c_{i,j+2} = 2t_{f_k}$, $c_{i,j+3} = 3t_{f_k}^2$, $c_{i,j+4} = 4t_{f_k}^3$, $c_{i,j+5} = 5t_{f_k}^4$, $c_{i,j+7} = -1$.
Acceleration: $c_{i+1,j+2} = 2$, $c_{i+1,j+3} = 6t_{f_k}$, $c_{i+1,j+4} = 12t_{f_k}^2$, $c_{i+1,j+5} = 20t_{f_k}^3$, $c_{i+1,j+8} = -2$.
Jerks: $c_{i+2,j+3} = 6$, $c_{i+2,j+4} = 24t_{f_k}$, $c_{i+2,j+5} = 60t_{f_k}^2$, $c_{i+2,j+9} = -6$.
Jounces: $c_{i+3,j+4} = 24$, $c_{i+3,j+5} = 120t_{f_k}$, $c_{i+3,j+10} = -24$.

The coefficients of the equations that connect the last with the first postural configurations are determined similarly. The elements of the $\mathbf{b}$ vector include the initial and final position values, i.e. q_{0_k} and q_{f_k}, and zeroes for the equations that are related to matching time derivatives. Overall, there are 27 joints that are moving and the same process is repeated for each one of them.

5. Reconstruction of Gait Cycle

5.1. Gait constraints

In order to reconstruct the gait cycle, one must constrain the human motion with the ground and specific gait parameters. First, it is necessary to include an inertial reference frame. The origin was chosen to be located on the ground, where the CM would project when the displacements of all the joint displacements of the human model are equal to zero. The z-axis is normal to the ground plane and the x-axis points along the line of progression. The interaction between the joint displacements and the ground, relative to the inertial reference frame, is carried out depending on specific events of the gait cycle; for example, the stance foot must be on the ground and gait parameters, such as the step width and foot angle, must be preserved. Therefore, each foot must satisfy some placement conditions (herein referred to as gait constraints) in every event of the gait cycle. Each gait constraint is used to create a function of the error distance between the desired position of a gait constraint and its actual position of the form $f_i = (x_{d_i} - x_i)^2$, where x_i represents the actual position of a postural configuration point that has to be approximated to some desired value x_{d_i}. The position of x_i is evaluated with the node points that were used to enclose the surfaces of the 3D human model. If a specific x_i does not correspond directly to an existing node point, a vector description was established.

https://doi.org/10.1017/S0263574711000440 Published online by Cambridge University Press

Table II. Gait constraints at the beginning of each period of the gait cycle.

		Right leg						Left leg						
Period	Name	Heel contact	Toes contact	Step width	Foot angle	Foot elevat.	Vert. tibia	Heel contact	Toes contact	Step width	Foot angle	Foot elevat.	Vert. tibia	Feet adjacent
I	Loading response	×		×	×				×	×	×			
II	Initial single stance	×	×	×	×				⊙	×	×			
III	Midstance	×	×	×	×							×		×
IV	Terminal stance	×	×	×	×							×	×	
V	Push off		×	×	×			×		×	×			
VI	Initial swing		⊙	×	×			×	×	×	×			
VII	Midswing					×		×	×	×	×			×
VIII	Terminal swing					×	×	×	×	×	×			

Table II shows the gait constraints that are employed in each event, where the symbol × indicates the occurrence of the event. A particular case is presented with the *Toes Contact* event, where the symbol × represents the full contact between the plantar surface of the toes with the ground, whereas the symbol ⊙ is used to indicate that only the tip of the toes is touching the ground.

The definition of each gait constraint is given next. *Heel Contact* describes the contact between the heel and the ground. The gait constraint that satisfies this condition is the vertical component of the heel centre being equal to zero, i.e. $x_{d_i} = 0$. *Toes Contact* may occur in two different forms: all the plantar surface of the toes being flat on the ground or only the tip of the toes touching the ground. Therefore, the forefoot is modelled with three node points – one node point representing the tip of the foot and the other two node points representing the axis of the MTP joint. If the vertical component of all three node points equals zero, the entire surface of the forefoot will remain in contact with the ground, as during the *midstance* period; whereas, if only the vertical component of the node point that represents the tip of the foot equals zero, then the foot would be seen as rolling about this point as during the *push off* period. When a node point must remain in contact with the ground, the desired value of the gait constraint is set to $x_{d_i} = 0$. *Step Width* is the lateral distance between the heel centres of two consecutive foot contacts and normally ranges between 7–9 cm.[23] In this work, the step width is measured relative to the line of progression (x-axis) and each heel centre is separated by 4 cm, i.e. $x_{d_i} = \pm 0.04$, where the $\pm$ sign indicates the left or right heel. *Foot Angle* is the angle between the line of progression and the longitudinal axis of the foot with 7° being considered as normal,[23] i.e. $x_{d_i} = \pm 7^\circ$. *Foot Elevation* represents the rise off the ground of the swinging foot, and this variable is included here to avoid the foot grazing the ground during the swing phase. This value varies during the swing phase between 2–5 cm and the distance is measured from the closest node point of the swinging foot to the ground. *Vertical Tibia* is determined by evaluating how close the tibia is from being vertical. The tibia represents a vector between the knee and ankle joints, the event occurs when the vertical component of the vector is reasonable close to the length of the tibia bone, i.e. $x_{d_i} = l_{sh}$, where l_{sh} is the length of the shank. *Feet Adjacent* occurs when the first component of the swinging heel

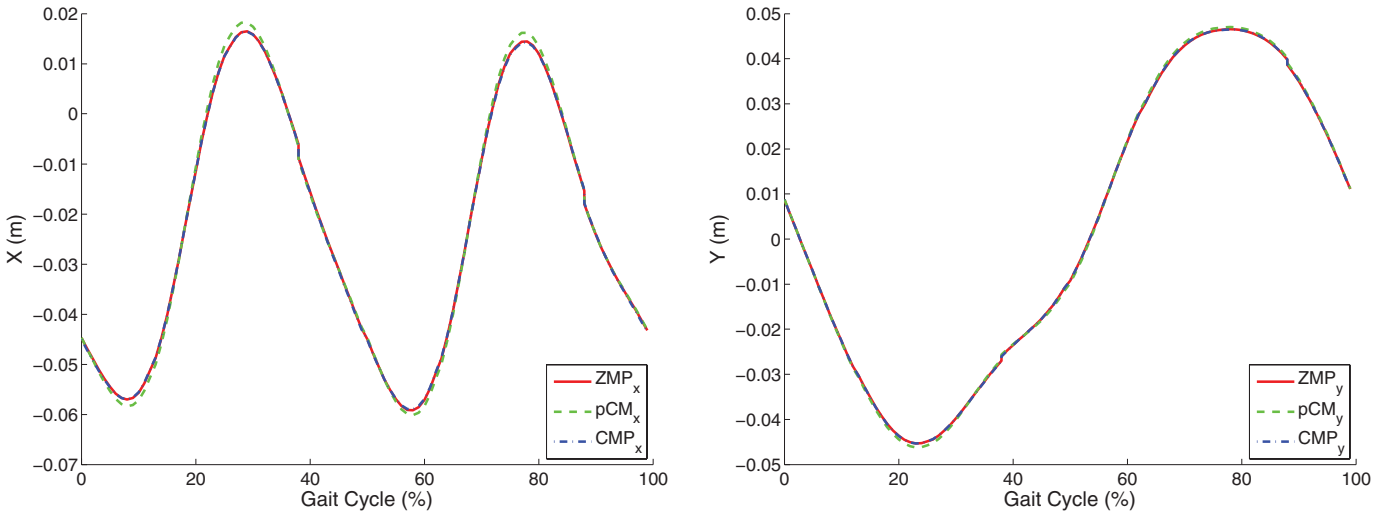

Fig. 3. (Colour online) Quasi-static Motion: profiles of ground reference points during gait cycle.

https://doi.org/10.1017/S0263574711000440 Published online by Cambridge University Press

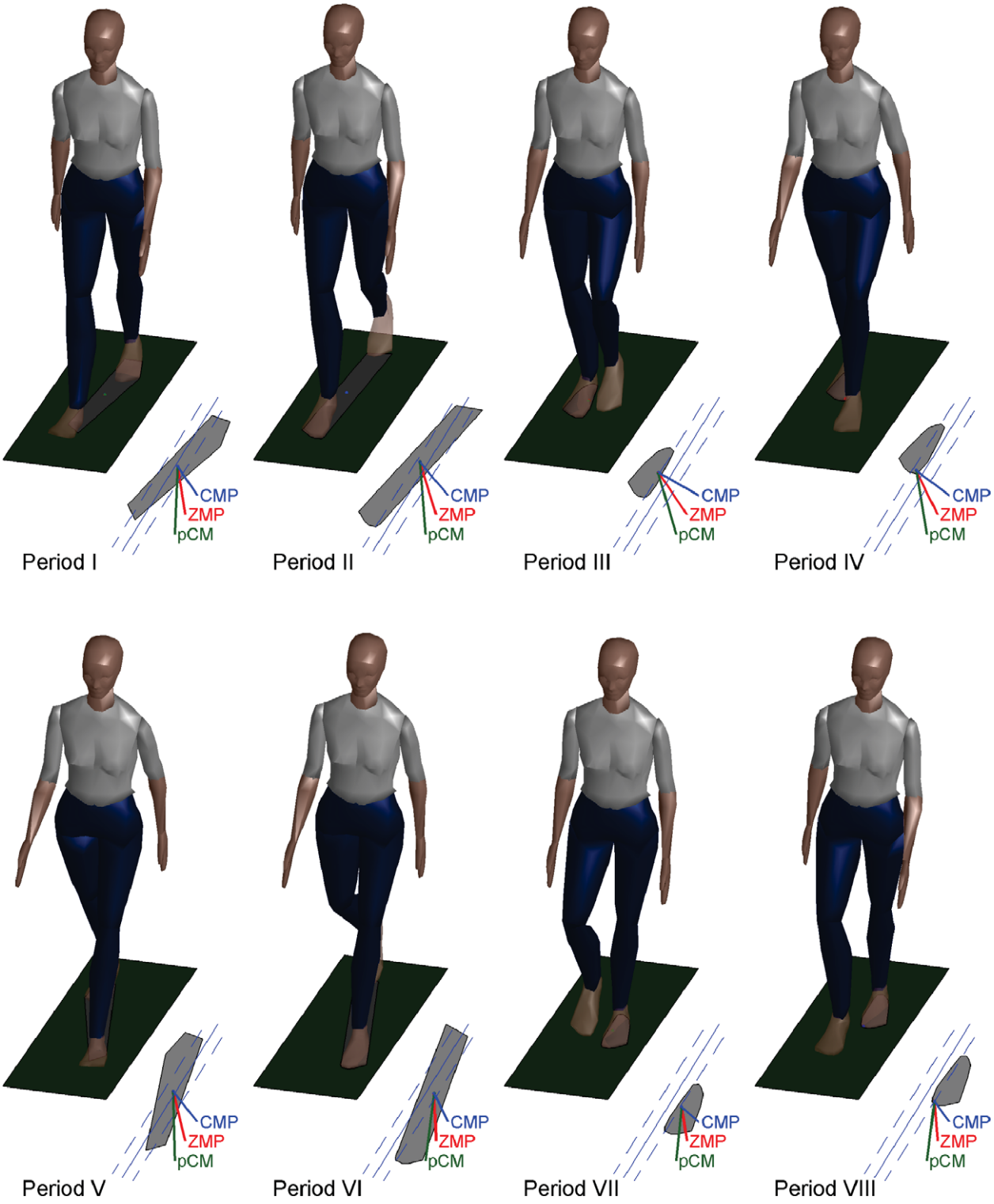

Fig. 4. (Colour online) Postural gait configurations during quasi-static motion.

centre coincides with the first component of the stance heel centre.

5.2. *Balance constraints*

The proposed human gait reconstruction process is based on a two-step optimisation method. In the first step, quasi-static motion is assumed. Since the gravitational forces are considerably greater than the inertial forces, all GRP would follow the same profile. Therefore, the pCM is considered as the variable that has to be approximated to a desired profile. Balanced profiles of the pCM during the gait cycle are reported in ref. [23]. For the second step, inertial forces/moments affect the postural stability during dynamic motion; therefore, the computed ZMP is approximated to a dynamically balanced CoP profile. For either optimisation step, a function of the error distance between the dynamically balanced profile (p_d) and the GRP variable (p) of the form $g_i = (p_d - p)^2$ is established.

https://doi.org/10.1017/S0263574711000440 Published online by Cambridge University Press

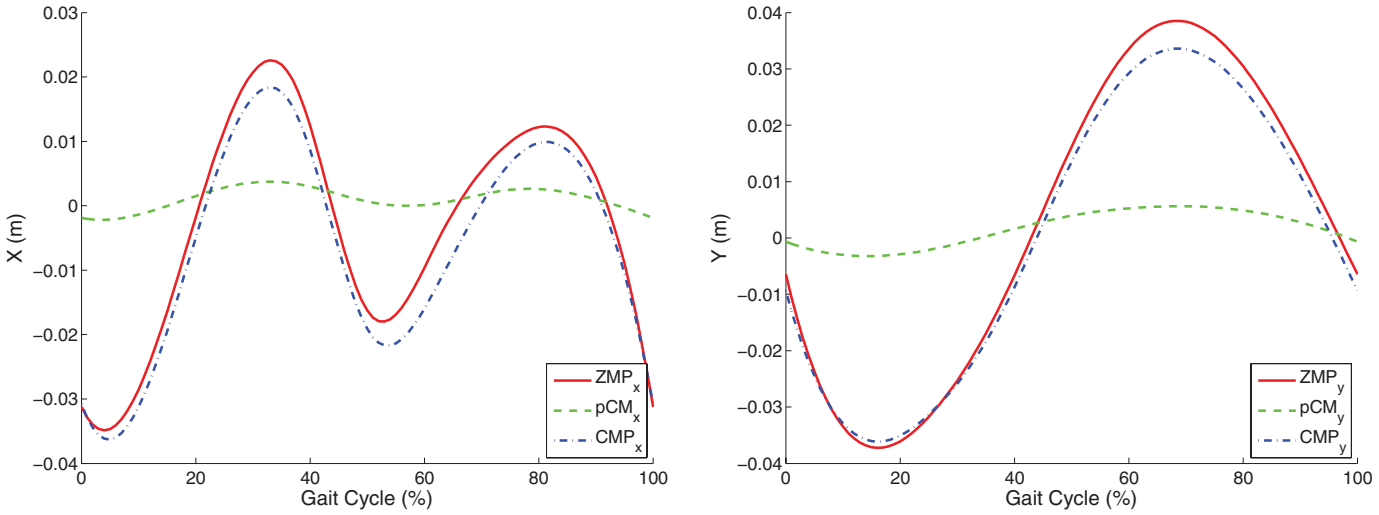

Fig. 5. (Colour online) Dynamic motion: profiles of ground reference points during gait cycle.

5.3. Optimisation problem

A two-step optimisation problem is used to generate the eight postural configurations that define the sequence of the dynamically balanced gait cycle. The method initially manipulates the postural configurations generated with the standard kinematic data by including gait and balance constraints under quasi-static conditions. This creates new postural configurations that can be used as the 'initial guess' for the second optimisation step. This is a highly non-linear problem due to the large number of design variables (joint displacements); thus, it is expected for the optimisation-based approach to modify the variables unequally, this would result in unnatural movements of the human gait. By including the first optimisation step, the resulting postural configurations are closer to the target solution, and therefore, the natural movements of the gait cycle are preserved.

For either optimisation step, an objective function that involves the gait and balance constraints is given as follows:

$$\text{minimise}\, f(\boldsymbol{\theta}) = \int \left(\sum \mu_i (x_{d_i} - x_i)^2 \; + \; \eta (p_d - p)^2 \right) \mathrm{d}t, \tag{6}$$

where μ_i and η are weighting functions.

6. Results

6.1. Quasi-static human gait

In the first optimisation step, the gait analysis is carried out with the treadmill assumed to be moving at a very low speed (10 steps/min). Given that the location of the CM is not a function of the velocities and accelerations of the body segments, then each postural configuration can be determined independently. This leads to a sequential process of postural configurations that involves 27 joints or design variables. The complete trajectory for each joint is subsequently generated. The optimisation problem is solved using a gradient-based algorithm (`fminsearch`).

Figure 3 illustrates the profile of the ground reference points. The results show that all the ground reference points are coincident throughout the gait cycle.

Figure 4 illustrates the postural gait configurations through the eight gait events, including the support polygon (the shaded area). Below each 3D postural gait configuration, the support polygon is re-drawn to indicate in a clearer manner the location of the ground reference points. The solid and dashed lines illustrate the direction of the line of progression and the step width (the distance between the dashed lines), respectively.

6.2. Dynamic human gait

For the second optimisation step, the sequential process carried out in the previous section cannot be used under dynamic conditions because the velocities and accelerations of the body segments are a function of the complete set of postural configurations. In other words, the ZMP is evaluated with inertial forces and moments (i.e. body segment velocities and accelerations). These velocities and accelerations are determined with the quintic polynomial splines, whose coefficients are a function of the complete set of postural gait configurations (via points); therefore, if one of the postural gait configurations is modified independently, the complete set of body segment velocities and accelerations that connect the other postural configurations will be altered as well, affecting the location of the ZMP in every configuration. Thus, an analysis of independent body postures cannot be carried out.

As an alternative, an optimisation technique that deals with this type of time-varying structure problems can be used instead. Bessonet *et al.*[29] proposed the use of parametric optimisation and four postural gait configurations. Herein, 'spacetime constraints,' an optimisation method used in computer graphics to provide more realistic motions to animations,[8] are employed. In biomechanics, Brogan *et al.*[30] employed spacetime constraints to optimise the trajectory of a passive-dynamic walker moving downwards on an inclined plane. The idea behind the spacetime constraint method is to treat kinematic constraints as consequences of force related effects. A special feature of this method is that the optimisation problem is formulated for the entire time period of the gait cycle. Consequently, for the eight events that occur within the complete cycle, there will be 27 (variables

https://doi.org/10.1017/S0263574711000440 Published online by Cambridge University Press

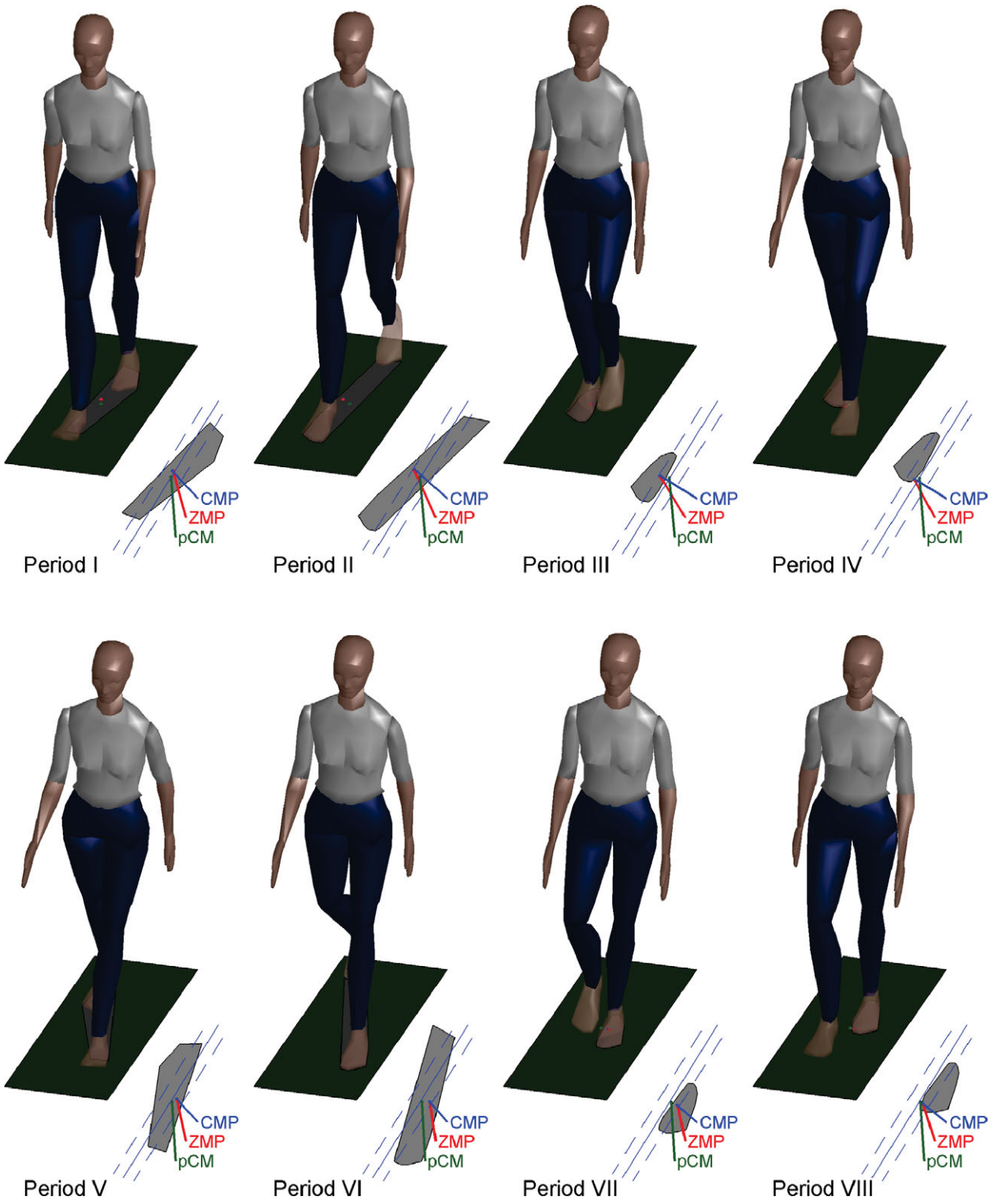

Fig. 6. (Colour online) Postural gait configurations during dynamic motion.

per postural gait configuration) × 8 (configurations) = 216 variables.

Due to the complexity of this problem, a gradient-based optimisation algorithm would be prone to finding local minima. Therefore, simulated annealing, which is a generic global optimisation algorithm, is used. The initial values entered in the algorithm are the 216 joint displacements found with the quasi-static solution (the combination of all postural configurations). The trajectory generator algorithm is performed at the beginning of every step of the optimisation technique, creating new sets of velocities and accelerations that are used to determine the location of the ZMP.

Figure 5 presents the profile of the three ground reference points. As expected, the amplitude of the pCM profile was reduced towards the line of progression, indicating that the upper body has to move less along the medio-lateral direction. Conversely, the ZMP and CMP profiles continue to be very close. Popovic *et al.*[19] also found that during normal

https://doi.org/10.1017/S0263574711000440 Published online by Cambridge University Press

Fig. 7. (Colour online) Paths of the nineteen optical markers (experimental).

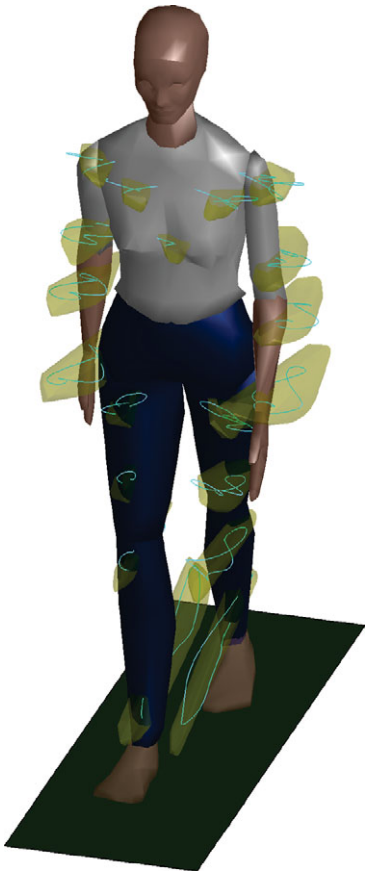

Fig. 8. (Colour online) Simulated trajectories that lie within the convex hull of the corresponding experimental paths.

gait, the CMP closely tracks the ZMP, i.e. the human body modulates the angular momentum during steady walking.

Figure 6 shows the dynamic postural gait along with the support polygon during the eight gait events. In all the events, the ZMP and CMP are contained within the boundaries of the support polygon. Conversely, the pCM exits the support polygon. The solid and dashed lines illustrate the line of progression and the step width, which are separated by 4 cm.

6.3. Experimental results

Experiments were conducted with a healthy individual walking on an instrumented treadmill (Bertec Coorporation). Both belts of the treadmill were set to move equally at 1.2 m/s. The motion of the subject was captured at a rate of 50 Hz using an active optical motion capture system (Visualeyez VZ3000, Phoenix Technologies, Inc.). Nineteen active LED markers were positioned on the body, which included three markers on the trunk and two markers on each thigh, shank, upper arm and forearm.

Following the experiment, the collected position data were processed by extracting 12 sequential gait cycles that did not show any type of perturbation, i.e. in all these cycles the subject maintained the rhythm of the treadmill speed. Figure 7 shows the paths followed by the 19 markers over the 12 cycles. Despite extracting unperturbed data, notice how all these cycles show slightly different patterns in Fig. 7.

The 3D human model was scaled in relation to the longitudinal body segment lengths to match the anthropometric parameters of the subject. Figure 8 illustrates the path followed by the node points of the 3D model that correspond to the location in which the LED markers were positioned. The semi-transparent volumes that surround these paths are the convex hull of all the experimental paths obtained from the optical LED markers.

Overall, the simulated trajectory is mostly contained within the convex hull of the experimental marker paths. The path followed by these points is very similar to the experimental paths on the sagittal plane. On the coronal plane, the profiles of the arm node points show a little more curvature than in the experimental results. This problem could have been caused in part by a more pronounced translation along the medio-lateral direction but also by the difference of arm swings between the subject of the original gait kinematic data and the subject who performed our experiments.

7. Discussion

One of the objectives of this work was to synthesise 3D human gait based on generic gait kinematics that were obtained from different literature sources and therefore were not related to our biomechanical model. Due to differences in the attachment of reference frames and body segment dimensions between our biomechanical model and the

https://doi.org/10.1017/S0263574711000440 Published online by Cambridge University Press

generic gait kinematics data, the resulting motion did not follow a proper gait pattern, in particular, for the feet/ground interaction. Nevertheless, these generic gait kinematics gave each body segment a natural movement. Thus, the objective was to slightly modify these initial joint displacements by incorporating balance and gait constraints and optimising the postural configurations with the proposed two-step method. As a result, a natural dynamically balanced set of trajectories was generated. This approach can be useful for rehabilitation purposes, where the abnormal gait pattern of a patient can be compared to optimal reference trajectories that are obtained with a patient-tailored model.

It is worth mentioning that although the amplitude of the pCM profile was reduced during the dynamic motion, there is still a visible medio-lateral translation in Fig. 6. As shown in Fig. 8, the path followed by the optical markers attached to the upper arms and trunk exited the convex hull of the corresponding experimental paths in this direction. One way to reduce this translation would be to include a second balance constraint involving the pCM following a predefined path in the optimisation problem.

Currently, our research group is developing a full-body measurement system based on miniature inertial/magnetic sensors that will be used for this purpose.[31] Our long term goal in this project is to employ this framework for the clinical online/offline analysis of postural stability of human subjects. Particular attention will be given to abnormal gait patterns that could lead to falls in frail older adults. By monitoring the dynamic gait activity of older adults in real-time, the cause and circumstances of falls will be investigated.

8. Conclusions

In this work, the development of a comprehensive framework for the analysis and synthesis of 3D dynamic human gait was presented. A detailed human body model consisting in 17 body segments, connected with 34 internal DOF, was employed. A realistic morphological 3D model of the human body was developed to visually validate human motion and to detect the interaction between the human body and the ground. The gait cycle is divided into eight postural gait configurations. The complete trajectory was generated with quintic polynomial splines.

Postural gait was reconstructed based upon standard gait kinematics and optimisation, with the objective function being the error distance between evaluated and desired gait/balance constraints. The gait constraints are related to the interaction of the plantar surface with the ground, step width, foot angle, etc. The balance constraints are defined by dynamically balanced GRP profiles. A two-step optimisation technique was used to generate dynamically balanced postural configurations. In the first step, gait constraints are introduced and the postural configurations are optimised under slow walking conditions (quasi-static motion). In the second step, normal speed gait (dynamic motion) and the effects of inertial forces/moments are considered. This problem is solved using the spacetime constraint method and a global optimisation algorithm. Experiments were conducted to validate the path followed by the generated reference trajectories. The results indicate that the path followed by the node points on the 3D model is mostly contained within the convex hull of 12 cycles of the optical marker paths.

Acknowledgements

The authors would like to thank Dr. Max Donelan and Dr. James Wakeling of Simon Fraser University for allowing them to access the Bertec instrumented treadmill and the PTI Visualeyez optical motion capture system. Also, the authors would like to thank Mr. Amr Marzouk and Dr. Iman Ebrahimi for helping with the experimental data collection.

References

1. D. A. Winter, *Biomechanics and Motor Control of Human Movement*, 4th ed. (John Wiley and Sons, Inc., Toronto, ON, Canada, 2009).
2. G. Bessonnet, J. Marot, P. Seguin and P. Sardain, "Parametric-based dynamic synthesis of 3D-gait," *Robotica* **28**(4), 563–581 (2010).
3. O. Khatib, E. Demircan, V. De Sapio, L. Sentis, T. Besier and S. Delp, "Robotics-based synthesis of human motion," *J. Physiol. Paris* **103**, 211–219 (2009).
4. M. Vukobratovic, H. Herr, B. Borovac, M. Rakovic, M. B. Popovic, A. Hofmann, M. Jovanovic and V. Potkonjak, "Biological principles of control selection for a humanoid robot's dynamic balance preservation," *Int. J. Hum. Robot.* **5**(4), 639–678 (2008).
5. J. Vermeulen, B. Verrelst, D. Lefeber, P. Kool and B. Vanderborght, "A real-time joint trajectory planner for dynamic walking bipeds in the sagittal plane," *Robotica* **23**(6), 669–680 (2005).
6. J. Perry, *Gait Analysis: Normal and Pathological Function* (SLACK Inc., Thorofare, NJ, USA, 1992).
7. A. Dasgupta and Y. Nakamura, "Making Feasible Walking Motion of Humanoid Robots from Human Motion Capture," *Proceedings of the 1999 IEEE International Conference on Robotics and Automation,* Detroit, MI, USA (May 10–15, 1999) pp. 1044–1049.
8. A. Witkin and M. Kass, "Spacetime constraints," *Comput. Graph.* **22**(4), 159–168 (1988).
9. V. M. Zatsiorsky, *Kinematics of Human Motion* (Human Kinetics, Windsor, ON, Canada, 1998).
10. F. Firmani and E. J. Park, "A Comprehensive human-body dynamic model towards the development of a wearable exoskeleton for paraplegics," *Trans. Can. Soc. Mech. Eng.* **33**(4), 745–758 (2009).
11. W. Mayol, B. Tordoff and D. Murray, "Designing a Miniature Wearable Visual Robot," *Proceedings of the 2002 IEEE International Conference on Robotics and Automation,* Washington, DC, USA (May 11–15, 2002) pp. 3725–3730.
12. V. M. Zatsiorsky, V. N. Seluyanov and L. G. Chugunova, "Methods of Determining Mass-Inertial Characteristics of Human Body Segments," **In:** *Contemporary Problems of Biomechanics* (G. G. Chemyi and S. A. Regirer, eds.) (Mir Publishers, Moscow; CRC Press, Boca Raton, FL, USA, 1990) pp. 272–291.
13. P. De Leva, "Adjustments to Zatsiorsky-Seluyanov's segment inertia parameters," *J. Biomech.* **29**(9), 1223–1230 (1996).
14. J. J. Craig, *Introduction to Robotics: Mechanics and Control*, 1st ed. (Addison-Wesley, Don Mills, ON, Canada, 1989).
15. D. A. Winter, *A.B.C. (Anatomy, Biomechanics and Control) of Balance During Standing and Walking* (Waterloo Biomechanics, Canada, 1995).
16. M. Vukobratovic and B. Borovac, "Zero-moment point – Thirty five years of its life," *Int. J. Hum. Robot.* **1**(1), 157–173 (2004).

https://doi.org/10.1017/S0263574711000440 Published online by Cambridge University Press

17. P. Sardain and G. Bessonnet, "Forces acting on a biped robot, center of pressure – Zero moment point," *IEEE Trans. Syst. Man Cybern. Part A Syst. Humans* **34**(5), 630–637 (2004).
18. A. Goswami and V. Kallem, "Rate of Change of Angular Momentum and Balance Maintenance of Biped Robots," *Proceedings of the 2004 IEEE International Conference on Robotics and Automation,* New Orleans, LA, USA (Apr. 26–May 1, 2004) pp. 3785–3790.
19. M. B. Popovic, A. Goswami and H. Herr, "Ground reference points in legged locomotion: Definitions, biological trajectories and control implications," *Int. J. Robot. Res.* **24**(12), 1013–1032 (2005).
20. T. Zielinska, C.-M. Chew, P. Kryczka and T. Jargilo, "Robot gait synthesis using the scheme of human motions skills development," *Mech. Mach. Theory* **44**(3), 541–558 (2009).
21. T. Saidouni and G. Bessonnet, "Generating globally optimised sagittal gait cycles of a biped robot," *Robotica* **21**(2), 199–210 (2003).
22. M. Whittle, *Gait Analysis: An Introduction* (Butterworth-Heinemann, London, UK, 2002).
23. D. A. Neumann, *Kinesiology of the Musculoskeletal System: Foundations for the Physical Rehabilitation* (Mosby, St. Louis, MO, USA, 2002).
24. L. Zhao, L. Zhang, L. Wang and J. Wang, "Three-Dimensional Motion of the Pelvis During Human Walking," *Proceedings of the 2005 IEEE International Conference on Mechatronics and Automation,* Niagara Falls, ON, Canada (Jul. 29–Aug. 1, 2005) pp. 335–339.
25. J. Simon, L. Doederlein, A. McIntosh, D. Metaxiotis, H. Bock and S. Wolf, "The Heidelberg foot measurement method: Development, description and assessment," *Gait Posture* **23**(4), 411–424 (2006).
26. C. Sartor, G. Alderink, H. Greenwald and L. Elders, "Critical kinematic events occurring in the trunk during walking," *Hum. Mov. Sci.* **18**(5), 669–679 (1999).
27. R. Shadmehr and S. P. Wise, *The Computational Neurobiology of Reaching and Pointing* (MIT Press, Cambridge, MA, USA, 2005).
28. C. Chevallereau and Y. Aoustin, "Optimal reference trajectories for walking and running of a biped robot," *Robotica,* **19**(5), 557–569 (2001).
29. G. Bessonnet, P. Seguin and P. Sardain, "A Parametric optimization approach to walking pattern synthesis," *Int. J. Robot. Res.* **24**(7), 523–536 (2005).
30. D. C. Brogan, K. P. Granata and P. N. Sheth, " Spacetime Constraints for Biomechanical Movements," *Proceedings of the Applied Modelling and Simulation,* Cambridge, MA, USA (Nov. 4–6, 2002) pp. 67–72.
31. J. K. Lee and E. J. Park, "Minimum-order Kalman filter via vector selector for human body orientation estimation," *IEEE Trans. Robot.* **25**(5), 1196–1201 (2009).

https://doi.org/10.1017/S0263574711000440 Published online by Cambridge University Press